

Microstructural characterization of SiC ceramic and SiC–metal active metal brazed joints

P. Prakash ^{a,*}, T. Mohandas ^a, P. Dharma Raju ^b

^a Defence Metallurgical Research Laboratory, Metal Joining Group, Kanchanbagh Post, Hyderabad, Andhra Pradesh 500058, India

^b Department of Metallurgical Engineering, NIT, Warangal, Andhra Pradesh 506004, India

Received 26 October 2004; received in revised form 7 January 2005; accepted 20 January 2005

Available online 13 March 2005

Abstract

SiC ceramic is joined to itself, to stainless steels and to Inconel 718 using indigenously developed active brazing alloys. Detailed interfacial product analysis by scanning electron microscopy, electron probe microanalysis and X-ray diffraction revealed that the interfacial reactions are dependent on Ti concentration and the composition of the metal member in the ceramic–metal couple. © 2005 Acta Materelia Inc. Published by Elsevier Ltd. All rights reserved.

Keywords: Brazing; EPMA; XRD; Ceramic; Ceramic–metal joints

1. Introduction

Previous studies [1] by the authors (PP and TM) on active brazing of alumina ceramic to different metals such as AISI 304SS, AISI 316SS (0.4 wt.%Ti), Inconel 718 (0.75–0.9 wt.%Ti and ~53 wt.%Ni), C.P Ti (99 wt.%Ti) with indigenously developed 76.5 wt.%–Ag–22.3 wt.%Cu–1.2 wt.%Ti (Ag–Cu–Ti) active brazing alloy (ABA), revealed that the reactivity of titanium is dependent on the metal member. This particular observation is in conformity with that reported by Vianco et al. [2] and Raymundo and Eagar [3]. In this present work, the authors attempt to study the effect of metal substrate composition on the interfacial reaction when SiC is used as the ceramic member employing the same Ag–Cu–Ti filler alloy. In addition, the effect of Ti concentration in the filler alloy and the effect of solvent of the brazing alloy is also investigated by carrying out brazing studies with indigenously developed 77.9 wt.%

Cu–17.25 wt.%Ag–4.26 wt.% Ti (Cu–Ag–Ti) ABA. The joining of engineering ceramics such as Al_2O_3 , Si_3N_4 and AlN to themselves and to metals is well reported. However, available data are scarce on the joining of SiC ceramics [4–9] compared to other engineering ceramics and the majority of the SiC joining studies are confined to either SiC–SiC joining [6,7] or to SiC–simple metal systems like Ti [5] and Ni/Cr/Ni–Cr [8,9]. Thus, detailed work on SiC joining with some of the familiar structural materials such as AISI 304SS, Inconel 718 etc. is not extensively reported, and the present work is an attempt to fill this gap.

2. Experimental methods

The SiC employed is supplied by International Advanced Research Centre for Powder Metallurgy & New Materials (ARCI), Hyderabad, in hot isostatic pressed condition. The ceramic and the metal members are employed as 5 mm thick discs. The nominal compositions of the metal members employed in this study are presented in Table 1. The two types of ABA employed

* Corresponding author. Tel.: +91 402 458 6605; fax: +91 402 434 1439.

E-mail address: suramprakash@rediffmail.com (P. Prakash).

Table 1

Nominal composition of base metal members (in wt.%)

Metal	C	Mn*	P*	S*	Si	Cr	Ni	Mo	Ti	Fe	Others
Type 304	0.08	2	0.045	0.03	1.00	18–20	8–10.5	–	–	Balance	–
Type 316	0.08	2	0.045	0.03	1.00	16–18	10–14	2–3	0.4	Balance	–
Inconel 718	0.64	–	–	–	–	18.5	Balance	3	0.75–0.9	18.5	Nb-5-1, Al-0.5

* Maximum values.

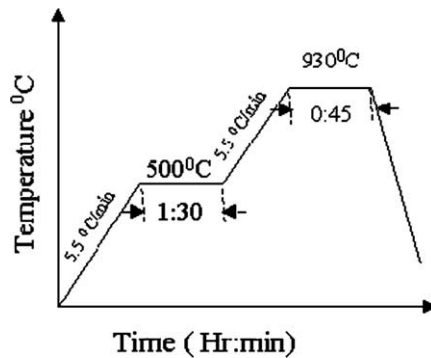


Fig. 1. Brazing cycle.

are 100 μm thick foils, produced in-house. More details about the process adopted in the manufacture of these ABA alloys is published elsewhere [10]. All the samples were polished on 800-grit paper, then cleaned with acetone, followed by etching with suitable acids and finally ultrasonically cleaned with acetone. Samples were then brazed in a high-vacuum brazing furnace with maximum temperature capability of 1200 $^{\circ}\text{C}$ at a vacuum of 10^{-6} mbar. A constant dead weight of 20 g was placed over the ceramic/metal assembly to ensure proper alignment during brazing. All the samples were brazed as per the brazing cycle shown in Fig. 1. Brazed samples were subsequently cross-sectioned using an ISOMET diamond saw, for metallographic characterization using optical, scanning electron microscope (SEM), electron probe microanalysis (EPMA) and X-ray diffraction (XRD) techniques.

3. Results and discussions

For convenience, the joints SiC–AgCuTi–SiC, SiC–CuAgTi–SiC, SiC–AgCuTi–AISI 304SS, SiC–Ag–CuTi–AISI 316SS, SiC–AgCuTi–Inconel 718 and SiC–CuAgTi–AISI 304SS are designated as S1, S2, S3, S4, S5 and S6, respectively. The back scattered electron (BSE) image and EPMA X-ray image analysis of joint S1 (Fig. 2) clearly reveals the Ti diffusion and build up at ceramic-filler alloy and filler alloy–metal interfaces, which is intended, indicating the efficacy of indigenously developed brazing alloy (Ag–Cu–Ti). Although preliminary investigation from the X-ray image analysis (Fig. 2) and from the works reported earlier on SiC,

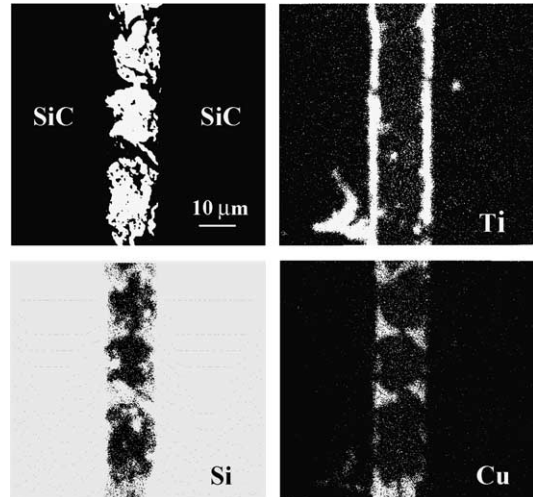


Fig. 2. BSE and X-ray image analysis of SiC–AgCuTi–SiC joint.

shows that the interfacial layer can be expected to comprise TiC [5,7], Ti–Si [5,6], Cu–Si and Cu–Ti (Fig. 2) compounds, the XRD pattern of joint S1 shown in Fig. 3 clearly indicates the presence of only two phases namely TiC and Cu_3Ti . The absence of Ti–Si compounds, is attributed to either the difference in the relative concentration of Ti available or to the process condition employed in the earlier works or to both these two factors. For example Naka et al. [5] had reported the formation of Ti_5Si_3 and $\text{Ti}_5\text{Si}_3\text{C}_x$, in which SiC is diffusion bonded to SiC using pure Ti (>95 wt.%Ti) foil as interlayer, whereas in the present study the Ti concen-

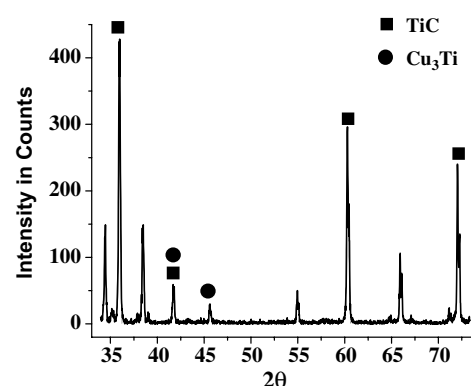


Fig. 3. XRD pattern of SiC–AgCuTi–SiC joint.

tration in the filler is as low as 1.25 wt.%. In addition, the joining temperature is also higher (1100–1500 °C) in their work [5], than in the present work (930 °C). The diffraction pattern of SiC–CuAgTi–SiC (S2), joined at 1050 °C, owing to the higher melting point of Cu–Ag–Ti ABA (950 °C) compared to that of Ag–Cu–Ti (772 °C) ABA [10], is akin to that of S1, suggesting that the change in Ti concentration (1.25–5 wt.%) or the change in the solvent of the brazing alloy does not have an effect on the interfacial product of SiC–SiC joint.

Fig. 4 shows the BSE and X-ray image analyses of SiC–AgCuTi–AISI 304SS joint (S3). Comparison of X-ray images of Cr, Fe and Ti clearly shows that Cr and Fe had diffused from the stainless steel through the active brazing alloy matrix (Ag–Cu) to the SiC interface, prior to the diffusion of active element Ti, as is evident from the clear shift in the segregation of Cr and Fe towards SiC, over which Ti had segregated. Thus, as can be predicted from the above observations, the XRD pattern of this joint shown in Fig. 5, shows that the interfacial reaction products consists of Cr_{23}C_6 as the major phase together with CrSi_2 , $\text{Cr}_{1.75}\text{Ni}_{0.25}\text{Ti}$, Cr_5Si_3 and FeSiC . Notably TiC is not observed in the XRD pattern, although the EPMA compositional analysis of this joint shown in Fig. 6 shows a possibility of a TiC phase about 4 μm wide. Nevertheless, Cr_{23}C_6 and Cr_5Si_3 are identified as the major phases in this system, although the presence of TiC is not completely ruled out. This

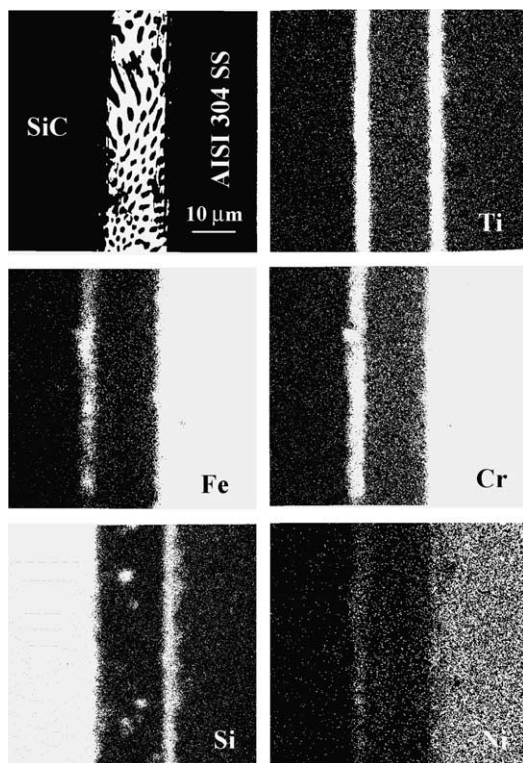


Fig. 4. BSE and X-ray image analysis of SiC–AgCuTi–AISI 304SS joint.

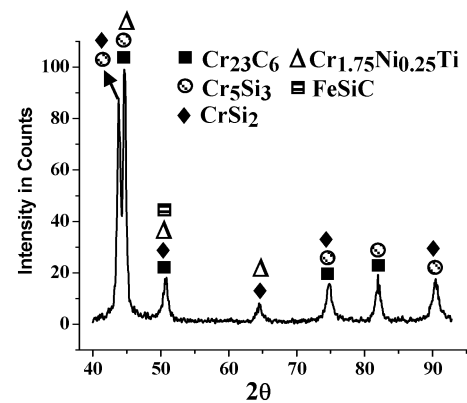


Fig. 5. XRD pattern of SiC–AgCuTi–AISI 304SS joint.

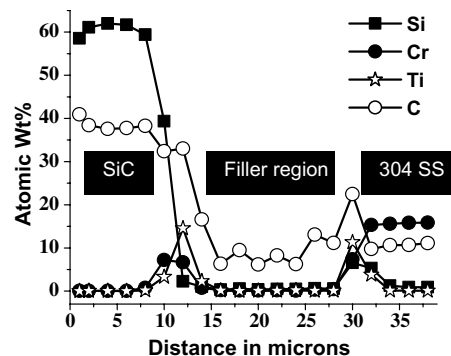


Fig. 6. EPMA compositional analysis of SiC–AgCuTi–AISI 304SS joint.

is well in conformity with the observations of Jackson et al. [8], in which SiC is diffusion coupled to Cr, who reported the presence of several carbide phases including Cr_{23}C_6 and Cr–Si compounds. Moreover the high negative free energy values (in kJ/mol) of Cr_{23}C_6 (−1634.879) [11] compared to TiC (−247.092) [12] at the brazing temperature employed in this study (930 °C) and the higher concentration of Cr (18 wt.%) available than the Ti availability (1.25 wt.%) further substantiates our current claim that in this particular system, Cr proactively reacts with SiC to form Cr_{23}C_6 and Cr–Si phases. The absence of expected Ti–Si compounds is attributed to the same reasons as explained for joint S1. Although the spatial occurrence of these phases is not clear from the XRD pattern, Fig. 6, it is possible to suggest that the interface product at SiC side comprises of Cr_{23}C_6 , FeSiC , Cr_5Si_3 and CrSi_2 while the stainless steel interface comprises a complex $\text{Cr}_{1.75}\text{Ni}_{0.25}\text{Ti}$, together with Fe and Si, though the latter is not identified in XRD.

In order to understand the effect of the presence of the active element Ti in the metal member on the interfacial reactions, SiC is joined to Ti stabilised AISI 316SS (0.4 wt.%Ti) using the same Ag–Cu–Ti filler alloy (S4). As expected, the chemistry of interfaces is found to be different from that of joint S3. Fig. 7 shows the XRD

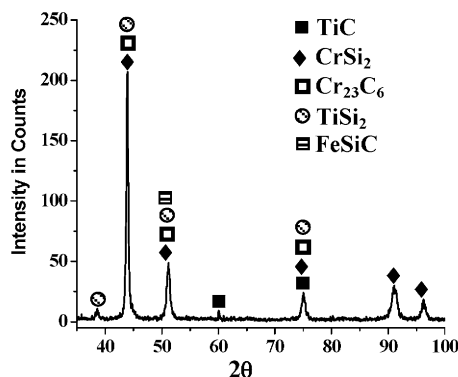


Fig. 7. XRD pattern of SiC–AgCuTi–AISI 316SS joint.

pattern of joint S4. In addition to Cr_{23}C_6 , CrSi_2 and FeSiC as in joint S3, two more expected phases namely TiC and TiSi_2 are also observed, although the amount of TiC phase is expected to be less from its weak signal intensity. The EPMA line scans of this joint (S4) shown in Fig. 8 further substantiates the presence of some of these phases, particularly to that of TiSi_2 . Thus an additional availability of Ti from the metal member had introduced the expected TiSi_2 and TiC phases which is absent in joint S3 (bare stainless steel), justifying the earlier reasoning for the absence of these compounds in SiC–AgCuTi–AISI 304SS joint (S3), owing to the lower concentration of Ti (1.25 wt.%) available in S3.

It was observed by Prakash et al. [1] that the presence of Ni as the major phase in the metal member (Ni based

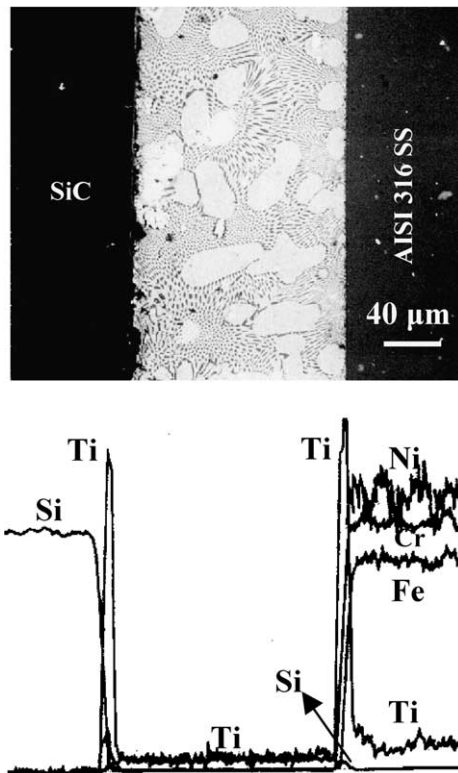


Fig. 8. BSE and EPMA line scan of SiC–AgCuTi–AISI 316SS joint.

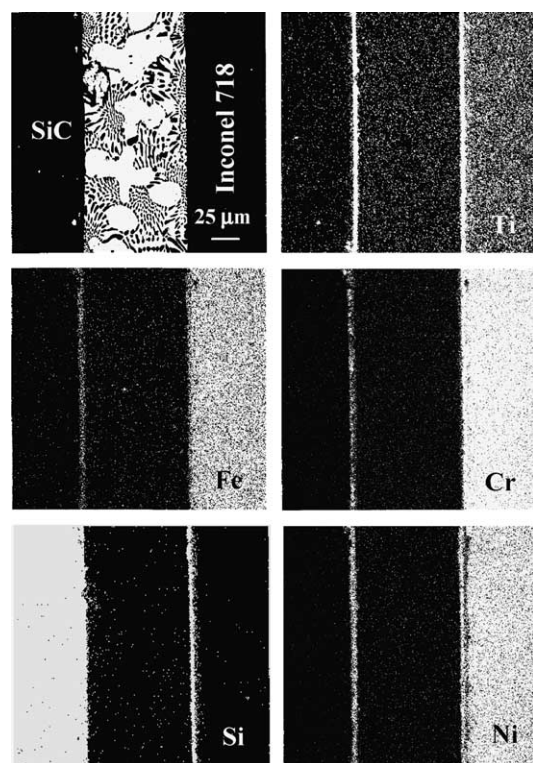


Fig. 9. BSE and X-ray images of SiC–AgCuTi–Inconel 718 joint.

alloys) had a pronounced effect in the joining of Al_2O_3 using the same filler Ag–Cu–Ti filler. A detailed study of the above will be published elsewhere. In this work, the same is attempted with SiC ceramic. Fig. 9 shows the BSE and EPMA image analyses of SiC–AgCuTi–Inconel 718 (S5) joint. Here again, as in joint S3, elements such as Cr , Fe and Ni had diffused from Inconel 718 side to SiC interface, whilst Si had diffused towards Inconel 718 from SiC. The XRD pattern of this joint, shown in Fig. 10, clearly identifies the presence of Cr_{23}C_6 , CrSi_2 as in joint S3, together with phases namely TiC , $\text{Ni}_{16}\text{Ti}_6\text{Si}_7$ and CuNi_2Ti . XRD pattern also shows Ti_3S_4 , Cr_5Si_3 (not identified in XRD) as minor phases. Evidently the predominant presence of TiC in this joint is clearly due to the higher Ti concentration available in this particular joint (1.25 + 0.8 wt.% Ti) compared to joints S3 (1.25 wt.% Ti) and S4 (1.25 + 0.4 wt.% Ti). Thus the above sequential experiments reveal that the chemistry of the interfaces can be well tailored according to the mechanical property requirements or to the application, by altering the chemical composition of the metal members, if the same is permissible. For instance, the active element (Ti) concentration in the brazing alloy can be kept as low as possible, at the same time sufficient bonding can be achieved by supplementing the active element from the metal member, thereby avoiding the brittleness problem generally encountered in the making of active brazing alloys with higher Ti concentration. Moreover, in the higher Ti concentration alloys, the unreacted Ti which remains in the alloy makes the alloy

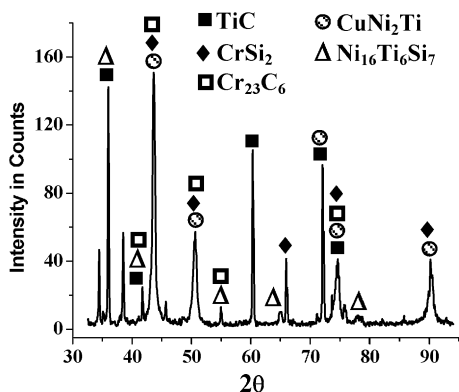


Fig. 10. XRD pattern of SiC–AgCuTi–Inconel 718 joint.

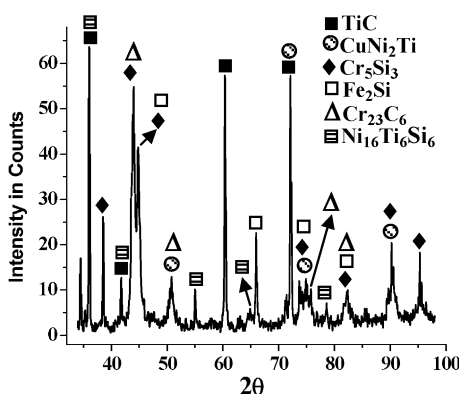


Fig. 11. XRD pattern of SiC–CuAgTi–AISI 304SS joint.

brittle, thereby hampering the stress relaxation functioning of the braze matrix (Ag–Cu). The above view is further rationalized when SiC is joined to AISI 304SS with Cu–Ag–4.25 wt.%Ti as filler (S6). The XRD pattern of this joint shown in Fig. 11 clearly shows the presence of TiC in the interface, attributed to the higher Ti concentration (4.25 wt.%) available in this particular joint than S3. Other major phases observed are Cr₂₃C₆, Cr₅Si₃, CuNi₂Ti, Ni₁₆Ti₆Si₇ and Fe₂Si.

4. Conclusions

(i) In SiC–AgCuTi–AISI 304SS joint, interestingly Cr₂₃C₆ is observed as the major phase and the expected TiC phase is notably absent. However, supplementing 0.4 wt.%Ti (from Ti stabilized AISI 316SS, as in SiC–AgCuTi–AISI 316SS joint) and 0.8 wt.%Ti (from Inconel 718, as in SiC–AgCuTi–Inconel 718) in addition to the 1.25 wt.% Ti present in the filler alloy (Ag–Cu–Ti) has introduced the TiC phase as the minor and major phases, respectively, in addition to the Cr₂₃C₆ phase. In SiC–CuAgTi–AISI 304SS (4.5 wt.%Ti in the filler

alloy) too, TiC is observed as the major phase in addition to Cr₂₃C₆. This tendency clearly shows that in addition to the filler alloy, the active element Ti can also be supplemented through the metal member to aid bonding.

- (ii) Strong presence of Cr₂₃C₆ phase in SiC–AgCuTi–AISI 304SS joints suggests that Cr can act as an effective active element in joining SiC to stainless steels, in which case conventional Ag–Cu brazing alloy can well be used instead of active brazing alloy, since stainless steel can provide Cr present in it during brazing. But the same has to be verified. In general the study has revealed that both Ag–Cu–Ti and Cu–Ag–Ti ABA are suitable for joining SiC to SiC, and SiC to metal combinations.
- (iii) In SiC to metal joints, the presence of Ni in the metal member does not influence the reactivity of active element Ti as observed in Al₂O₃ to metal joints in our earlier studies.

Acknowledgements

The authors are grateful to DRDO for funding this programme. The authors wish to express their gratitude to Dr. A.M. Sriramamurthy, Director, DMRL for his invaluable support and keen interest in this work. One of the authors (PP) wishes to thank sincerely Mr. V.V. Ramarao, Scientist'D', SFAG, DMRL for his help in imparting training on the operation of EPMA. Authors are also thankful to Mr. V. Ramakrishna TO'B' and Mr. M. Yadagiri TO'A' of XRD Section, SFAG, DMRL, for their support in carrying out XRD analysis.

References

- [1] Prakash P, Mohandas T, Ramarao VV. In Proc National symp on vacuum science and technology and vacuum metallurgy, IVSNS-2003, BARC, Mumbai, 2003. p. 451.
- [2] Vianco PT, Stephens JJ, Hlava PF, Walker CA. Welding J 2003;9:252-S.
- [3] Raymundo A, Eagar TW. Acta Mater 2003;51:4871.
- [4] Liu HJ, Feng JC, Qian YY. Scripta Mater 2000;43:49.
- [5] Naka M, Feng JC, Schuster JC. Metall Mater Trans A 1997;28A:1385.
- [6] Nishino T, Urai S, Okamoto I, Naka M. J Mater Sci Lett 1990;9:1417.
- [7] Tamai T, Naka M. J Mater Sci Lett 1996;15:1025.
- [8] Jackson MR, Mehan RL, Davis AM, Hall EL. Metall Mater Trans A 1983;14A:355.
- [9] Feng JC, Liu HJ, Naka M, Schuster JC. Mater Sci Tech 2003;19:137.
- [10] Prakash P, Mohandas T, Ramarao VV, Narasimha Rao K. DMRL TR 2003. vol. 341, 2003. p.20.
- [11] Barin I. Thermochemical data of pure substances, Part I. 2nd ed. Germany: VCH; 1993. p. 425.
- [12] Barin I. Thermochemical data of pure substances, Part II. 2nd ed. Germany: VCH; 1993. p. 1528.